Formation and Characterization of an Aqueous Zirconium Hydroxide Colloid

Peter D. Southon,*,† John R. Bartlett,‡ James L. Woolfrey,‡ and Besim Ben-Nissan†

Department of Chemistry, Materials and Forensic Science, University of Technology, Sydney, Australia, and Materials Division, Australian Nuclear Science and Technology Organisation, Sydney, Australia

Received April 22, 2002. Revised Manuscript Received June 24, 2002

Among the wide variety of routes reported for the chemical synthesis of zirconia, the development of simple, aqueous sol−gel technology is of considerable interest for industrial-scale applications. In this study, zirconium hydroxide nanoparticles were produced by the controlled hydrolysis of zirconium carbonate in nitric acid, followed by gentle heating at 70 °C. Transparent, colorless gels were subsequently produced from the concentrated sols (500 g/L, oxide basis) by drying at ambient temperature. The nanoparticle sols and gels were characterized using a range of techniques, including EXAFS, Raman spectroscopy, dynamic light scattering, and SAXS, which revealed the presence of platelike particles of width 2.8 ± 0.4 nm and thickness 0.5 ± 0.1 nm. The platelets exhibit a surprisingly high degree of short-range ordering, and it is demonstrated that they are composed of stacked layers of two-dimensional "$[Zr(OH)_4]_n$" sheets, as proposed (but not established) in earlier studies. The speciation of the nitrate anions in the sols was also investigated by Raman and ^{14}N NMR, which revealed that the majority of anions were closely associated with the nanoparticles (i.e., separated from the surface by several layers of coordinated water molecules), rather than coordinated directly to the surface. The role of such species in maintaining the stability of the nanoparticle sols is discussed.

Introduction

The chemical synthesis of ceramic precursor powders from solution has been an area of considerable interest for several decades. The thermodynamics and kinetics of such methods are very different from those prevailing in traditional high-temperature ceramic processing, frequently leading to novel compositions and structures and excellent control over homogeneity, porosity, crystal size, and so forth.[1]

Many routes for the solution-based preparation of zirconia sols, gels, films, and powders have been reported in the literature, using inorganic and metal−organic precursors, aqueous and nonaqueous media, and a range of methods (e.g., precipitation and hydrothermal processing), yielding materials with a wide range of properties and potential applications. Although many of these routes have been extensively studied, there are still unresolved questions. Some of these questions are related to the short-range structure of any intermediate "amorphous" phase that is formed during synthesis, the reactions by which this structure is formed, its relationship to the structure of the precursor chemicals, and its influence over the relative stability of the tetragonal and monoclinic phases in the zirconia product.

Aqueous routes for the synthesis of ceramics could be particularly suitable for large-scale processes due to the absence of harmful solvents. Although a number of aqueous routes for the processing of zirconia have been reported and used, little research has been published over the past decade. Aqueous routes in general have been largely eclipsed by the strong interest in routes using metal−organic precursors, which offer greater control over the hydrolysis reactions. Aqueous sols and gels for the synthesis of zirconia are usually prepared from precursor zirconium salt solutions by forcing hydrolysis to occur, either chemically or thermally, so that colloidal particles of an hydroxide or oxide are formed. Gels are most simply prepared by rapidly adding base to a zirconium salt solution, while stable colloidal dispersions can be prepared by hydrothermal treatment of a zirconium salt solution.

This paper examines a very simple method of forcing hydrolysis in a controlled way and forming a colloid at relatively low temperature, first reported in the patent literature.[2] The method involves the addition of further zirconium (in the form of a hydroxide or carbonate) to an acidic zirconyl nitrate solution, to give a $Zr:NO_3$ ratio of 1:1. The decomposition of the added material consumes acid, promoting hydrolysis and polycondensation to form colloidal particles. The resultant sol will gel reversibly on evaporation of water or when the pH is raised, and irreversibly if the nitrate anions are re-

* To whom correspondence should be addressed. Present address: Department of Chemistry, University of Aberdeen, AB24 3UE, United Kingdom. E-mail peter.d.southon@uts.edu.au
† University of Technology, Sydney.
‡ Australian Nuclear Science and Technology Organisation.

(1) Rao, C. N. R. *Mater. Sci. Eng. B* **1993**, *18*, 1.

(2) Woodhead, J. L. United Kingdom Patent No. 1181794, 1970.

10.1021/cm0211913 CCC: $22.00
Published on Web 09/14/2002

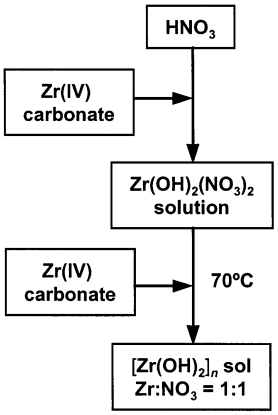

Figure 1. Method used to prepare the sol particles.

moved. This method has been mentioned occasionally in research literature,[3−5] but the structure of the sol particles has not previously been investigated.

This method is attractive for industrial applications for a number of reasons. All precursor materials are inorganic and commercially available, and the method is aqueous, simple, and rapid, with no hydrothermal processing required. The reversible gelation provides an extra degree of control over the forming process; misshaped products may be redispersed, and sols may even be gelled in bulk for storage and redispersed for processing.[3] The sol is stable for at least 4 years and can remain a fluid with an oxide content as high as 500 g/L (≈30 wt %), which is considerably higher than sols prepared by hydrothermal processing. These features result in the simplicity, ease of scale-up, low cost, and minimal environmental impact of the process.

To develop applications for this route and improve the process, it is important to understand in detail the structure of the sol particles and the reactions that occur as the sol is prepared. In investigating the structure and reactions, we have also elucidated some interesting aspects of aqueous zirconium chemistry.

Procedure

The method used to prepare the sol is illustrated in Figure 1.[2] One mole of hydrated zirconium carbonate (Magnesium Elektron, 43.6 wt % oxide) was dissolved in 2 mol of nitric acid, producing a transparent, highly acidic, zirconyl nitrate solution, $Zr(OH)_2(NO_3)_2$. A second mole of zirconium carbonate was mixed with water to form a slurry and slowly added to the solution with stirring over a period of ≈15 min. The mixture was maintained at 70 °C for 1−2 h, forming a nearly transparent sol with a final $Zr:NO_3$ ratio of 1:1. Samples of the zirconyl nitrate solution and the sol were diluted to 1.0 M and left for ≈1 week at ambient temperature before characterization. No aging effects were observed over this time, and the pH remained constant at ≈0.8. A small amount of the sol was placed in a glass dish and left under an airflow for several days to produce a hard, brittle, and transparent gel.

The size distribution of the nanoparticles at 30 °C was determined using dynamic light scattering (Nicomp Autocorrelator). Samples were diluted in water to ≈0.4 M, to reduce multiple scattering and interparticle effects, and then filtered through several 0.45-μm PTFE filters prior to analysis. Laser light of wavelength 488 nm was passed through the vial, and variations in the intensity of the scattered light were detected simultaneously at scattering angles of 39.8° and 79.5°. Scattering data from each angle were analyzed independently and the particle size distributions calculated using a proprietary Nicomp algorithm. Data collection times of 24 h were typically used.

The size and shape of the cations or particles in the solution and sol were characterized by small-angle X-ray scattering, using an instrument described in ref 6. The samples were contained in glass capillaries, and the same section of capillary was used for first the background (pure water) measurement and second the sample measurement. Scattering curves were obtained for the solution and several samples of the sol, each at 1 M concentration, and an additional sample was prepared by diluting the sol to 0.2 M. A $\ln(I)$ vs $\ln(q)$ plot of the data was used to identify the overall shape of the scattering particles. Theoretical scattering curves for a range of simple homogeneous shapes (sphere, plate, rod, and ellipsoid) were also fitted to the data, to determine the size and shape of the scattering particles. A least-squares fitting routine was used to refine the dimensions of the "model" particle to provide the optimum fit to the measured scattering curves. To minimize the effects of multiple scattering, the fitting procedure was applied only over the range $q > 0.15$ Å^{-1}, which was relatively free of such effects.

The FT Raman spectra of the solutions, sols, and gels were recorded at ambient temperature (Bio-Rad FT-Raman II). For the liquid samples the depolarization ratios (ρ) of the Raman bands were also determined. Bands with $\rho < 0.2$ were assigned as polarized, and those with $\rho > 0.7$ (theoretical maximum 0.75) were assigned as depolarized.

The ^{14}N NMR spectra of the solutions and sols were recorded on a Bruker-Spectrospin 300 DRX spectrometer at 21.69 MHz, using a pulse width of 17.4 μs. All samples were diluted to 0.2 M prior to analysis. Shifts were measured with respect to the position of the NH_4^+ resonance at −359.6 ppm in a saturated aqueous solution of ammonium nitrate.

X-ray absorption spectra of the gels were recorded at the Australian National Beamline Facility (ANBF), which is located at the Photon Factory synchrotron, Tsukuba Science City, Japan. The gel was ground finely, thoroughly mixed with boron nitride to produce a sample with optimum absorbance, and then pressed into a flat disk. The sample was held in a cryostat, and spectra were recorded in transmission mode, across the Zr K-edge, at 10, 80, and 290 K. The reference materials used were monoclinic zirconia and barium zirconate. Standard data processing and background-subtraction procedures were carried out using the X-FIT software package.[7] A theoretical single-scattering model, generated from the FEFF7 level theory,[8,9] was fitted simultaneously to the three Fourier-transformed spectra, using the FEFFIT software package.[10] A range of models were tested, with the most suitable being two nearest-neighbor "shells" of oxygen atoms, and two additional shells of zirconium atoms. The amplitude reduction factor was set at 0.9, consistent with the absorbance spectra of the reference materials, and also with previous studies.[11,12] The Debye−Waller disorder factor, σ^2, for each shell was split into a static component and a vibrational component. While the former (along with all other parameters) was set to be the same for each data set, the latter was allowed to vary between data sets, constrained by an Einstein-correlated model for

(3) Woodhead, J. L. *J. Mater. Ed.* **1984**, *6*, 887.
(4) Zhang, W.; Glasser, F. P. *J. Eur. Ceram. Soc.* **1993**, *11*, 143.
(5) Sizgek, E.; Bartlett, J. R.; Brungs, M. P. *J. Sol-Gel Sci. Technol.* **1998**, *13*, 1011.
(6) Aldissi, M.; Henderson, S. J.; White, J. W.; Zemb, T. *Mater. Sci. Forum* **1988**, *27/28*, 437.
(7) Ellis, P. A.; Freeman, H. C. *J. Synchrotron Radiat.* **1995**, *2*, 190.
(8) Rehr, J. J.; Mustre de Leon, J.; Zabinsky, S. I.; Albers, R. C. *J. Am. Chem. Soc.* **1991**, *113*, 5135.
(9) Ankoudinov, A. L. Relativistic Spin-dependent X-ray Absorption Theory; Ph.D. Thesis: University of Washington, 1996.
(10) Newville, M.; Ravel, B.; Haskel, D.; Stern, E. A.; Yacoby, Y. *Physica B* **1995**, *208 & 209*, 154.
(11) Haskel, D.; Ravel, B.; Newville, M.; Stern, E. A. *Physica B* **1995**, *208 & 209*, 151.
(12) Li, P.; Chen, I. W.; Penner-Hahn, J. E. *Phys. Rev. B* **1993**, *48*, 10063.

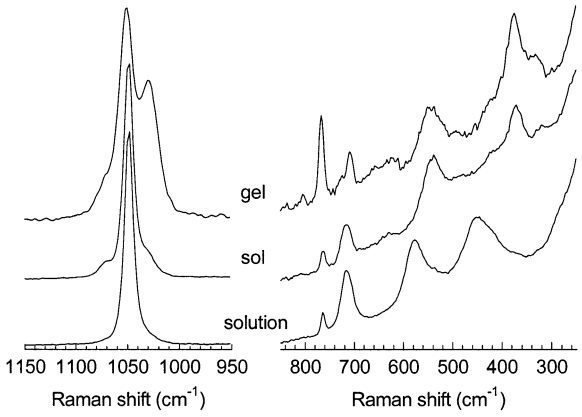

Figure 2. Raman spectra of the zirconyl solution, sol, and gel, over the ranges 950−1150 and 300−850 cm^{-1}.

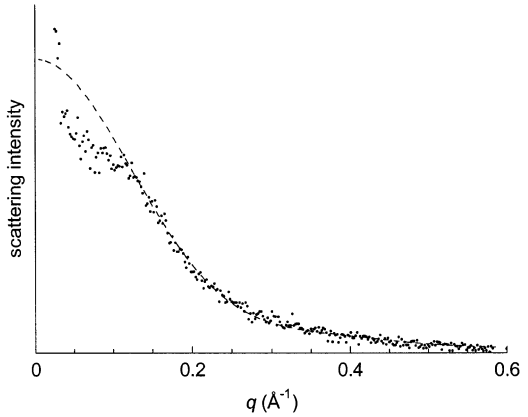

Figure 3. Typical X-ray scattering curve of the sol. The broken line represents the best fit for the cylinder model.

oxygen shells, or a Debye-correlated model for zirconium shells.[13] To reduce the number of variables in the model, values of σ^2 for the two oxygen shells were constrained to be equal.

To examine the sol particles by TEM, a diluted sol was coated onto a standard TEM carbon grid and dried. Bright-field images and electron diffraction patterns were measured with a JEOL 2000 FX analytical TEM. X-ray diffraction patterns of finely ground gel were measured with a Scintag X1 diffractometer using Cu Kα radiation.

Results and Discussion

Zirconyl Nitrate Solution. The intensity of light scattered through the zirconyl nitrate solution was negligible, indicating the absence of significant quantities of particles larger than ≈1 nm. The solution also scattered X-rays only very weakly. The small-angle X-ray scattering (SAXS) curve (not shown) was consistent with that of scattering by spherical particles and was best fitted by a sphere with a radius of gyration of 0.40 ± 0.04 nm and diameter 0.52 nm. These dimensions are very close to those previously reported for the cyclic-tetramer species, $[Zr_4(OH)_8]^{8+}$, in zirconyl chloride solutions.[14,15] Previous studies have determined that the cyclic tetramer predominates in concentrated (>0.1 M) chloride solutions,[14,16] and the present results strongly suggest that this species also predominates in the nitrate solution.

This conclusion is supported by the Raman spectrum of the zirconyl nitrate solution, shown in Figure 2, which has two main Raman bands below 650 cm^{-1}. Zirconyl chloride solutions also possess two broad Raman bands at similar positions (see Table 1),[17−19] which have been assigned to Zr−O vibrations within the bridging hydroxy groups.[17,18] We consider the same assignment to apply to the spectrum of the nitrate solution. The bands observed above 650 cm^{-1} are assigned to various vibrations of the nitrate anion, as discussed below.

Table 1. Positions and Polarization Assignments of Bands Observed in Raman Spectra <650 cm^{-1} [a]

$Zr(OH)_2Cl$ solution[18]	$Zr(OH)_2(NO_3)_2$ solution	sol	gel
		630 dp	630 ?
582 p	580 p	540 p	545
456 dp	450 dp	420 sh dp	430 sh
	420 sh dp	375 dp	375
			320 sh

[a] p = polarized; dp = depolarized; sh = shoulder.

Structure of the Sol Nanoparticles. The sols scattered light weakly, and the scattering characteristics of several sols of this type were examined. The particle-size distribution calculated from the dynamic light-scattering results showed that the vast majority of the scattering particles possessed a hydrodynamic diameter in the range 3−6 nm. Most samples also contained a small fraction of 10−20-nm particles, which accounted for up to 50% of the scattered light, but were calculated to make up <5% of the solids volume. Although particle-size distributions based on complex models must be treated with caution, data measured independently at the two angles gave very similar size distributions, lending weight to the analysis.

A typical X-ray scattering curve for the sol is shown in Figure 3. Note that the low-angle region of the curve is distorted due to interference between X-rays scattered from neighboring particles in a relatively concentrated sol; consequently, only the region $Q > 0.15$ $Å^{-1}$ was fitted. The curve was best fitted by a simple plate model, giving a plate size of 2.8 ± 0.4 nm wide × 0.5 ± 0.1 nm thick. The corresponding theoretical scattering curve is also shown in Figure 3 as a broken line. The scattering curve of a sol that had been diluted further to 0.2 M (not shown) showed less distortion at low angle, but scattered very weakly. Analysis of this curve gave similar results to the more concentrated sol.

These results can be contrasted against previously published SAXS studies of zirconyl salt solutions aged at temperatures between 80 and 100 °C over periods between 10 and 100 h,[20,21] which found that the initial particles formed were rod-shaped. This is clearly not the case here, and it is probable that the polymerization

(13) Dalba, G.; Fornasini, P. *J. Synchrotron Radiat.* **1997**, *4*, 243.
(14) Singhal, A.; Toth, L. M.; Lin, J. S.; Affholter, K. *J. Am. Chem. Soc.* **1996**, *118*, 11529.
(15) Toth, L. M.; Lin, J. S.; Felker, L. K. *J. Phys. Chem.* **1991**, *95*, 3106.
(16) Baes, C. F.; Mesmer, R. E. *The hydrolysis of cations*; Wiley-Interscience: New York, 1976.
(17) Burkov, K. A.; Kozhevnikova, G. V.; Lilich, L. S.; Myund, L. A. *Russ. J. Inorg. Chem.* **1982**, *27*, 804.
(18) Kozhevnikova, G. V.; Myund, L. A.; Burkov, K. A. *Izv. Akad. Nauk SSSR, Neorg. Mater.* **1988**, *24*, 470.
(19) Hannane, S.; Bertin, F.; Bouix, J. *Bull. Soc. Chim. Fr.* **1990**, *127*, 43.
(20) Singhal, A.; Toth, L. M.; Beaucage, G.; Lin, J.; Peterson, J. *J. Colloid Interface Sci.* **1997**, *194*, 470.
(21) Jutson, J. A.; Richardson, R. M.; Jones, S. L.; Norman, C. *Mater. Res. Soc. Symp. Proc.* **1990**, *180*, 123.

mechanism is affected by the very different reaction rates, and possibly the temperature and anion present.

The small discrepancy in the average particle "size" determined by the two techniques is due to the presence of surface hydroxy and nitrate groups, and a layer of bound water, all of which are included in the hydrodynamic diameter but have X-ray scattering characteristics very similar to those of the surrounding water matrix and thus are not detected by SAXS.

Vibrations of metal−oxygen bonds are generally found in the 200−650-cm^{-1} region, and the zirconyl nitrate solution, the sol, and the gel all have Raman spectra with two principle bands in this region. The positions and polarization assignments for all bands below 650 cm^{-1} are listed in Table 1. A comparison of the Raman spectra of the solution and sol in Figure 2 show that the bands below 650 cm^{-1} have been substantially shifted or replaced, indicating considerable changes in the short-range structure. The polarized 580- and 540-cm^{-1} bands, in the solution and sol spectra respectively, are assigned to a similar vibration that has been perturbed during the polymerization process, most probably the symmetric stretching of the bridging hydroxy groups. The EXAFS data discussed below shows that these bridging hydroxy groups survive in the sol particles, and it can be seen in Figure 2 that the Raman spectra of the sol and gel are very similar in the region below 650 cm^{-1}.

While not previously reported for nitrate solutions, similar changes in the Raman spectra have been observed in chloride solutions,[17,19,22−24] although the band at 375 cm^{-1} has not been previously reported. For example, Hannane, Bertin, and Bouix found that adding a base to zirconyl chloride replaced bands at 456 and 580 cm^{-1} with those at 426 and 533 cm^{-1}.[19,22] However, there has been no consensus as to the assignment of these bands. These spectra can also be compared to those published for a range of gelatinous precipitated zirconium hydroxides, which had a broad band at 450 cm^{-1}, while some also had a strong band at 550 cm^{-1}.[23]

Structure of the Gel. The structure of the particles in the sol can be further elucidated by studying the short-range order of the gel. It is probable that little change to the internal structure of the particles occurs during gelation; not only is gelation completely reversible, but also the Raman spectra of the sol and gel are very similar in the region below 650 cm^{-1}. The X-ray diffraction pattern of the gel (discussed below) shows only very broad peaks, indicating an absence of long-range order.

The values derived from the fitting of the EXAFS spectra provide a wealth of information on the short-range structure of the particles in the gel. Figure 4 shows the background-subtracted EXAFS spectrum of the gel, measured at 10 K, while the Fourier-transformed spectra, measured at 10, 80 and 290 K, are shown in Figure 5. Fourier-transformed EXAFS spectra are effective average pseudo-radial distribution functions of the atoms surrounding each zirconium atom.

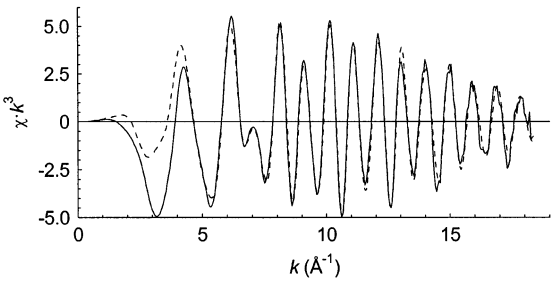

Figure 4. Weighted EXAFS spectrum of the gel, measured at 10 K (solid line), compared with the modeled spectrum (broken line).

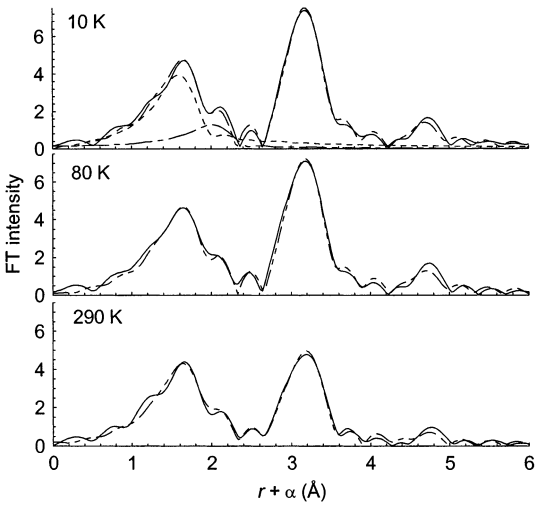

Figure 5. Fourier-transformed spectra of the gel, measured at 10, 80, and 290 K (solid line), compared with the modeled spectrum (broken line). The 10 K plot includes the modeled profiles for the individual oxygen shells.

Table 2. Structural Parameters from the Model Fitted to the EXAFS Spectrum of the Gel[a]

shell	distance from Zr atom (Å)	coordination number	σ^2_{10K} (Å$^2 \times 10^{-3}$)	σ^2_{290K} (Å$^2 \times 10^{-3}$)
O1	2.106(9)	7.6(6)	11(2)[b]	12(2)[b]
O2	2.58(2)	4.2(6)	11(2)[b]	12(2)[b]
Zr1	3.539(3)	3.8(2)	3.6(3)	5.6(3)
Zr2	4.995(9)	1.9(8)	5(2)	8(2)

[a] Note: The uncertainty in the last digit is indicated in parentheses. [b] Disorder parameters for O1 and O2 were set to be equal to reduce the number of modeling parameters.

The first peak is assigned to the "nearest-neighbor" oxygen atoms immediately adjacent to the zirconium atom, while the next two peaks are attributed mainly to nearby zirconium atoms.

The modeled interatomic distances, coordination numbers, and disorder parameters for each shell are listed in Table 2. The temperature dependence of the disorder parameter, σ^2, are listed for measurements made at 10 and 290 K. From these parameters the short-range structure of the particles in the gel has been determined.

The parameters for the zirconium shells indicate the nature of the Zr−Zr framework. Each zirconium atom is coordinated by approximately four other zirconium atoms at a distance of 3.54 Å. The next shell of zirconium atoms is at 5.00 Å, which is exactly $\sqrt{2}$ times the first-shell distance. This is good initial evidence that the zirconium atoms are positioned in a square, two-dimensional lattice in which the Zr−Zr distance for the

(22) Hannane, S.; Bertin, F.; Bouix, J. *Bull. Soc. Chim. Fr.* **1990**, *127*, 50.
(23) Tosan, J.-L.; Durand, B.; Roubin, M.; Bertin, F.; Loiseleur, H. *Eur. J. Solid State Inorg. Chem.* **1993**, *30*, 179.
(24) Sharygin, L. M.; Galkin, V. M.; Vovk, S. M.; Korenkova, A. V. *Colloid J. USSR* **1985**, *47*, 95.

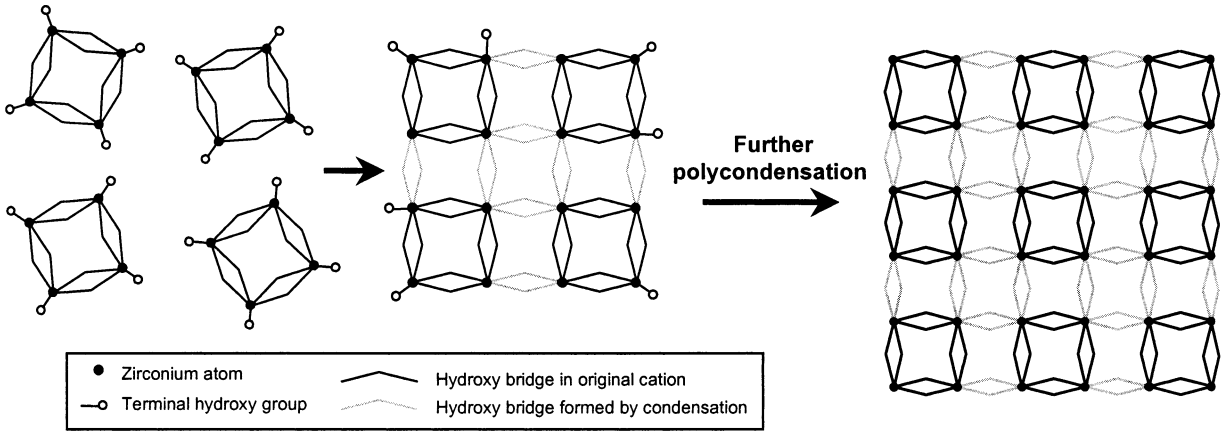

Figure 6. Schematic illustration of the condensation of four "cyclic tetramers" into an oligomer and then a platelike particle.

second shell of zirconium atoms represents the "diagonal" distance across the "square".

The presence in the first shell of approximately eight oxygen atoms surrounding each zirconium atom strongly indicates that most zirconium atoms are linked to their four zirconium neighbors by double hydroxy bridges; such bridges are common in aqueous zirconium species. The presence of coordinated nitrate groups will also contribute oxygen atoms to the first shell. As indicated below, the Raman spectrum of the gel indicates that ≈0.5 nitrate groups per zirconium are directly bidentate-coordinated to zirconium atoms; thus, an average of 1 oxygen atom out of the ≈8 observed will belong to a nitrate group.

A short-range structural model can now be proposed, in which zirconium atoms are arranged in a two-dimensional square lattice, each connected by double hydroxy bridges, as shown in Figure 6, giving an ideal stoichiometry of $Zr(OH)_4$. The hydroxide precipitated from salt solutions has also been shown to have this stoichiometry.[25] However, the lower than expected coordination numbers show that the sheet structure is not perfect, probably due to the edges of the sheet, defects in the lattice, and any oxo bridges present.

From the shape and size of the particles, as determined by SAXS, it seems reasonable that several of these sheets will be stacked together to form each particle. The second "oxygen" shell, at a distance of 2.58 Å from the central atom, can be assigned to oxygen atoms in adjacent sheets, coordinated water molecules, or nitrogen atoms in the coordinated nitrate groups, probably a combination of all three.

The nearest known structure to that proposed is the cyclic-tetramer cation, $[Zr_4(OH)_8]^{8+}$, which exists as a discrete unit in crystalline $Zr(OH)_2Cl_2 \cdot 8H_2O$.[26] The known distances for Zr−O(H), Zr−$(OH)_2$−Zr, and the diagonal Zr−Zr pair compare well with those distances proposed from this EXAFS study, lending further support for this model.

This two-dimensional $Zr(OH)_4$ structure has been previously suggested by Clearfield as a likely product of the polymerization of cyclic-tetramer units.[27] However, until now no clear experimental evidence has existed for the occurrence of $Zr(OH)_4$ in a square, two-dimensional lattice, and there have been few previous publications in which a detailed structure has been proposed for similar "amorphous zirconia" systems. A previous EXAFS study of an amorphous zirconia precursor found similar interatomic distances for the first shells of oxygen and zirconium that were consistent with a partially oxolated version of this structure,[28] but did not find the characteristic 5.0-Å Zr−Zr diagonal distance. This diagonal distance has only been reported once before, in a EXAFS study of an inorganic sol with a $Zr:NO_3$ ratio of 1:1, but very little detail accompanied this report.[29] All previous EXAFS studies of zirconia precursors have been carried out at ambient temperature, greatly increasing the uncertainties in the coordination numbers and disorder parameters.

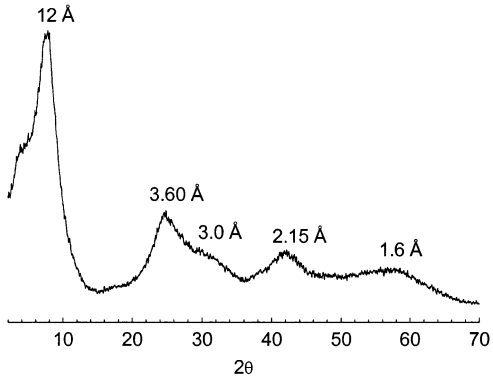

Figure 7. X-ray diffraction pattern of the gel, with approximate *d*-spacing values corresponding to the peaks.

A typical diffraction pattern of a ZN1.0 gel is shown in Figure 7. Although there are no sharp diffraction peaks corresponding to a crystalline phase, there are a number of broad peaks in the pattern that are reproducible and characteristic, with approximate *d* spacings at 12, 3.6, 3.0, 2.15, and 1.60 Å. None of these peaks correspond to crystalline zirconyl nitrate. The diffraction patterns of amorphous zirconia or zirconium hydroxide generally contain some very broad peaks,[30,31] but they

(25) Zaitsev, L. M. *Russ. J. Inorg. Chem.* **1966**, *11*, 900.
(26) Mak, T. C. W. *Can. J. Chem.* **1968**, *46*, 3493.
(27) Clearfield, A. *Rev. Pure Appl. Chem.* **1964**, *14*, 91.
(28) Turrillas, X.; Barnes, P.; Dent, A. J.; Jones, S. L.; Norman, C. J. *J. Mater. Chem.* **1993**, *3*, 583.
(29) Ramsay, J. D. F. *Synchrotron radiation, Appendix to the Daresbury annual report 1988/89*; Science and Engineering Research Council, 1989; p 38−39.
(30) Ward, D. A.; Ko, E. I. *Chem. Mater.* **1993**, *5*, 956.
(31) Turrillas, X.; Barnes, P.; Häusermann, D.; Jones, S. L.; Norman, C. J. *J. Mater. Res.* **1993**, *8*, 163.

are generally not as distinct as those observed for this gel. One similar diffraction pattern has been observed, for a gel prepared by refluxing a concentrated zirconyl chloride solution.[32]

The relatively intense peak at 12 Å is the easiest to interpret. Such "low angle" peaks are commonly found in the diffraction patterns of aggregates of colloidal particles and are indicative of the average distance between the particles. This value is consistent with face-to-face stacking of the particles in this gel. Given that the 5-Å-thick plate-shaped particles are stacked at an average separation of 12 Å, this allows for an approximately 3−4-Å layer of coordinated water and nitrate anions around each particle. In this case the stacking arrangement is not ordered enough to give rise to second- or third-order diffraction peaks.

The other peaks observed at higher angles cannot be indexed as a conventional diffraction pattern. However, X-ray scattering in nondiffracting materials also give rise to characteristic patterns, based on average interatomic distances. Although no detailed analysis has been made along these lines, it is interesting to note that the two main Zr−Zr and Zr−O(H) distances determined by EXAFS are quite close to two of the observed peaks.

Electron microscopy has the potential to further elucidate and confirm the structures described here. An early TEM study of an amorphous zirconia that had been obtained by refluxing a zirconyl chloride solution gave evidence for a very thin, coherent, amorphous film consisting of structural units 5−10 Å in diameter,[33] which is consistent with the structure reported here. However, there have been no subsequent studies reported. Our own attempts at obtaining high-resolution TEM images of the gel were not successful, and the electron diffraction patterns indicated that the gel was fairly susceptible to beam damage.

Location of the Nitrate Groups. It is also of interest to characterize the location and coordination of the nitrate species within the sol, as they may play a role in preventing the aggregation of the particles. Both ^{14}N NMR and Raman spectroscopy have been used to compare the environment of the nitrate groups in the solution and the sol.

The Raman bands observed above 650 cm^{-1} were assigned to nitrate groups with different symmetries, in accordance with the literature values for other metal−nitrate salts.[34] Two types of nitrate groups were identified: the fully aquated (ionic) nitrate group, with D_{3h} symmetry unaffected by other nearby molecules, and the bidentate-coordinated (chelating) nitrate ligand, with C_{2v} symmetry. The former has characteristic bands at 1046 and 720 cm^{-1}, while the latter has characteristic bands at 1025 and 766 cm^{-1}.

The Raman spectra above 650 cm^{-1} for the solution and sol are very similar; in both cases the most abundant nitrate species in the solution is the ionic species with D_{3h} symmetry, while the chelating species makes up only a small fraction. Thus, the symmetry of the nitrate groups is not affected by the formation of the colloidal particles. The only significant change in the region above 650 cm^{-1} with the increase in Zr:NO_3 ratio is the appearance of a new band at 1070 cm^{-1}, as a minor shoulder on the 1050-cm^{-1} peak. Unfortunately, we have not been able to assign this band.

In contrast, the ^{14}N NMR spectra of the solution (not shown) contains a single broad peak at ≈6 ppm, while for the sol no ^{14}N peak could be detected at all. Thus, in the formation of the sol, while the symmetry of most of the nitrate anions is not changed, their immediate environment is altered sufficiently to greatly perturb the NMR signal.

It is known that the quadrupolar ^{14}N nucleus is extremely sensitive to the proximity of cations in the immediate environment,[24] and its NMR signal may be strongly perturbed even if the nitrate species is not close enough to the cation to complex it. One possible mechanism is that the NMR relaxation time is increased to the extent that the NMR signal is no longer able to be detected.[35] Alternatively, nitrate groups that are strongly "associated" with a particle will spin at the same rate as the particle, which is much more slowly than a "free" nitrate species in solution; in this case the NMR signal will undergo quadrupolar broadening and may broaden out to be indistinguishable from the background. In either case, all of the nitrate species become "associated" with the zirconium species as the colloidal particles are formed, making them undetected by NMR. Note that a previous quantitative ^{14}N NMR study of zirconyl nitrate solution found that only about 50% of the nitrate anions in solution were able to be detected.[36]

One of the implications of this observation is that the liquid separating the particles will contain only a very low concentration of nitrate anions. Therefore, unlike with colloids in an electrolyte, there will be little screening of the charge on the double layer around the particles, thus promoting the stability of the sol.

With gelation a large fraction of the nitrate species change from ionic to chelating symmetry of the bidentate-coordinated nitrate. The bands at 715 and 1050 cm^{-1}, assigned to the ionic species, become much less intense with gelation, while the 766- and 1030-cm^{-1} bands, assigned to the chelating species, increase in intensity. By comparing the Raman spectrum with that of $Zr(OH)_2(NO_3)_2 \cdot 5H_2O$ crystalline salt, a structure that contains an equal number of ionic and chelating nitrate species,[37] it is estimated that the gel also contains an approximately equal abundance of these species.

Polymerization Mechanism. From the structure of the particles, we can now determine the reaction mechanism for their formation, based on the previously established aqueous chemistry of zirconium.[16,27] The decomposition/dissolution of 1 mol of zirconium carbonate in 2 mol of nitric acid forms a stoichiometric solution of zirconyl nitrate $Zr(OH)_2(NO_3)_2$. The aquated "zirconyl" cations contain no more than several zirconium atoms, and SAXS data presented above suggest that the cyclic-tetramer structure predominates. In these cations

(32) Matsui, K.; Suzuki, H.; Ohgai, M.; Arashi, H. *J. Am. Ceram. Soc.* **1995**, *78*, 146.
(33) Fryer, J. R.; Hutchison, J. L.; Paterson, R. *J. Colloid Interface Sci.* **1970**, *34*, 238.
(34) Nakamoto, K. *Infrared and Raman spectra of inorganic and coordination compounds*; Wiley-Interscience: New York, 1986.
(35) Pronin, I. S.; Vashman, A. A. *Russ. J. Inorg. Chem.* **1987**, *32*, 338.
(36) Livage, J.; Chatry, M.; Henry, M.; Taulelle, F. *Mater. Res. Soc. Symp. Proc.* **1992**, *271*, 201.
(37) Benard, P.; Louër M.; Louër, D. *J. Solid State Chem.* **1991**, *94*, 27.

each zirconium atom is connected to two neighboring zirconium atoms by double hydroxy bridges. The water molecules associated with these cations hydrolyze very readily, leading to the formation of reactive terminal hydroxy groups on the cations and a highly acidic solution.

When the additional mole of zirconium carbonate is fully dissolved in this solution, more polynuclear zirconyl species will be formed, most probably with structures similar to those of the cations already present. This reaction increases the pH, which will promote further hydrolysis. Condensation between the terminal hydroxy groups will be promoted by the increased abundance of these groups, the reduced average charge on the zirconyl species, and the increased concentration of the zirconyl species. The net result is to convert coordinated water molecules into hydroxy bridges between zirconyl species.

As condensation of the cations continues, oligomers will be formed that are large enough to be regarded as colloidal particles. One probable polycondensation process proposed by Clearfield is illustrated schematically in Figure 6,[27] which assumes that all of the initial cations present are cyclic tetramers. If the tetramers condense to form a square, two-dimensional oligomer, the zirconium atoms in the center are valance-satisfied and eight-coordinated, and so are relatively unreactive and unlikely to be involved in further hydrolysis. However, the water molecules at the edges of the oligomer continue to hydrolyze, and further condensation occurs at the edges. In this way the oligomer will grow as a sheet to form platelike particles with the short-range structure reported by EXAFS.

The scheme illustrated here is only very general, and other processes may well take place alongside the mechanism described. For instance, cyclic-tetramer cations may not necessarily polymerize in the ordered structure illustrated above, leading to disruptions in the two-dimensional lattice.[27] Further disruptions would be caused by the addition of zirconyl monomers, dimers, and so forth, to the growing oligomer or the joining of two growing oligomers.

The rate-limiting reaction in the polymerization process is most probably the decomposition of the zirconium carbonate. Because this is a relatively slow reaction, and the carbonate is evenly dispersed in the solution as it decomposes, the hydrolysis and polycondensation reactions also occur homogeneously through the solution so that colloidal particles are formed instead of a hydroxide gel precipitating out of solution.

Given that the average particle dimensions are 3-nm wide × 0.5-nm thick, and assuming a Zr−Zr spacing of 0.354 nm, we estimate that there are ≈50 zirconium atoms in each two-dimensional "sheet" and that most particles will contain between one and three such sheets. These sheets would be mostly bound by hydrogen bonds between hydroxy groups in adjacent layers. Some direct bonding, via hydroxy groups, is also possible between the layers. A small fraction of the nitrate species is directly bound to zirconium atoms on the surface of the particles. The remainder is aquated but located close to the particles, probably as counterions to any remaining positive charge. Water molecules are likely to be coordinated to at least some of the zirconium atoms, particularly those at the edge.

Conclusions

The formation of the nanoscale colloidal particles from the zirconyl nitrate solution involves controlled polycondensation between the zirconyl species, with the carbonate acting as a base to promote the reaction. A combination of characterization techniques has shown that the particles are plate-shaped, with a highly ordered two-dimensional '$Zr(OH)_4$' structure, conclusive evidence for which has not been previously reported. The nitrate anions in the sol are all closely associated with the particles, although most are not directly bound to them, which may contribute toward the remarkable stability of the sol.

Acknowledgment. We would like to thank Dr. Kim Finnie of ANSTO for her assistance in interpreting the Raman spectra, Trevor Dowling of Australian National University for assistance with collection of SAXS data, and Dr. Kamali Kanangara of UTS for collection of the ^{14}N NMR spectra. P.D.S. also acknowledges the support of an Australian Postgraduate Award from the Australian Government, a Postgraduate Research Award from the Australian Institute for Nuclear Science and Engineering, and the support of the Materials Division of the Australian Nuclear Science and Technology Organization. Access to the Photon Factory was provided by the Australian Synchrotron Research Program, which is funded by the Commonwealth of Australia under the Major National Research Facilities Program.

CM0211913